7. ODP LEG 116 SITE SURVEY[1]

Shipboard Scientific Party[2]

INTRODUCTION

The Leg 116 drill sites are located in the central Indian Ocean approximately 800 km south of Sri Lanka on the distal Bengal Fan (Fig. 1). The location is approximately halfway between the Indrani and Indira fracture zones on crust created in the Late Cretaceous by sea-floor spreading on the southeast Indian Ridge (Sclater and Fisher, 1974).

The drilling sites were chosen to be within a broad region of the central Indian Ocean that has undergone significant intraplate deformation (Eittreim and Ewing, 1972; Stein and Okal, 1978; Weissel et al., 1980), apparently beginning in the upper Miocene (Moore et al., 1974). The deformation has taken the form of long-wavelength (100–300 km) undulations or folds with peak-to-trough amplitudes of 1 to 3 km (Weissel et al., 1980; Geller et al., 1983) (Fig. 2). The deformation also takes the form of faulted and rotated blocks, 5 to 20 km wide superimposed on the long-wavelength undulations. Seismic reflection records show the top of the ocean crust to be, in places, offset by up to 0.5 s of two-way traveltime (>500 m) across these faults (Fig. 2). One of the major objectives of the Leg 116 drilling was to utilize the record of deformation, as recorded in the structures developed in the syn-deformation Bengal Fan sediments, to date the onset of deformation and the subsequent history of motion of a fault block.

The Bengal Fan, together with its eastern lobe, the Nicobar Fan, is the world's largest submarine fan (Curray and Moore, 1971; Emmel and Curray, 1984) covering an area of 3×10^6 km (Fig. 3). The Fan is 3000 km long, 800–1400 km wide, and over 16 km thick beneath the northern Bay of Bengal. The Leg 116 sites are located on the distal edge of the fan where the sediment thickness is 1.5 to 2 km (Fig. 4).

Even though it is perhaps the largest sedimentary feature on Earth, the Bengal Fan has not been extensively investigated. Fewer than 100 piston cores have sampled the surface sediments and, prior to Leg 116, only one DSDP site (Site 218, Leg 22) had been drilled into the fan. This site was located east of Sri Lanka at 8°N, more than 1000 km northeast of the Leg 116 sites. The sediment thickness at Site 218 was estimated as 3.5 to 4.0 km (Shipboard Scientific Party, 1974). Site 218 terminated at a depth of 773 m in mid-Miocene turbidites, but due to a combination of spot coring and poor recovery, only 54 m of sediment was recovered. The sediments recovered at Site 218 consisted of interbedded clean silts, sandy silts, clayey silts and silty clays of turbidite origin, with sporadic layers of clay-rich nannofossil ooze (Shipboard Scientific Party, 1974). Based on a grain-size analysis, the Shipboard Scientific Party (1974) suggested that four distinct pulses of turbidite activity have occurred since the middle Miocene. Moore et al. (1974) were able to assign a late Miocene age to the "Upper Unconformity" of Curray and Moore (1971), but the sparse recovery and poor fossil record prevented a more precise determination of its age. This "Upper Unconformity" appears to correlate with the unconformity marking the onset of intraplate deformation further south (Geller et al., 1983).

REGIONAL SETTING FOR LEG 116 SITES

The Leg 116 sites are located in 4735 m of water roughly halfway between the Indrani and Indira fracture zones (Fig. 1). These fracture zones were identified by Sclater and Fisher (1974) on the basis of magnetic anomaly offsets and in general do not have a bathymetric expression. The Afanasy Nikitin seamounts are located along the Indira fracture zone from about 2°S to 5°S. This elongated seamount edifice appears to be continuous over that distance and reaches depths of 3200 m on the few available crossings, but little else is known of this seamount group.

Figure 5 shows a series of north–south magnetic anomaly profiles located between the Indrani and Indira fracture zones (line locations shown in Fig. 6). The magnetic anomalies can be easily correlated with the model profile shown, which was generated using the LaBrecque et al. (1977) time scale with a spreading rate of 6 cm/yr. This anomaly identification essentially agrees with that of Sclater and Fisher (1974), although the V1909 profile is the only line that they had available between these two fracture zones. The 150-km offset of anomalies 30 to 33 between profiles INMO7 and V1909 sugests the presence of an additional fracture zone between those lines and indeed Sclater et al. (1976) do identify an additional fracture zone between the Indrani and Indira fracture zones south of 19°S. However, the situation is not that simple since the older anomalies, 33R and 34, are not offset by a similar amount. This could have resulted from a ridge crest jump between 72 and 76 Ma to create the fracture zone or by an episode of asymmetric spreading on one side of an already existing small fracture zone that served to increase the offset. The WI821 line crosses the Indira fracture zone near anomaly 33. Anomaly 33 may therefore be present twice on that profile.

The C2706 magnetic profile (Fig. 5) was collected during the site survey on the approach to and departure from the Leg 116 sites. The location of the Leg 116 sites is indicated on the profile. The sites are all located between anomalies 33R and 34, and comparison with the model profile implies that the crust beneath is 78 m.y. old.

Figure 7 shows north–south bathymetry lines located between the Indrani and Indira fracture zones (see Fig. 6 track locations). The long-wavelength intraplate deformation can be clearly seen as domal highs of a few hundred meters relief and 50 to 100 km width disturbing the otherwise smooth surface of the distal fan. These topographically elevated areas are characteristically spaced 200–300 km apart and correspond to gravity highs with an amplitude of 25–50 mgal (Fig. 8). The seismic reflection data available prior to the site survey is shown in Figure 9. The V2901 seismic profile passes directly over the Leg 116 sites. Both the long-wavelength undulations and the smaller scale faulting can

[1] Cochran, J. R., Stow, D.A.V., et al., 1988. *Proc. ODP, Init. Repts.*, 116: College Station, TX (Ocean Drilling Program).

[2] Shipboard Scientific Party is as given in the list of Participants preceding the contents.

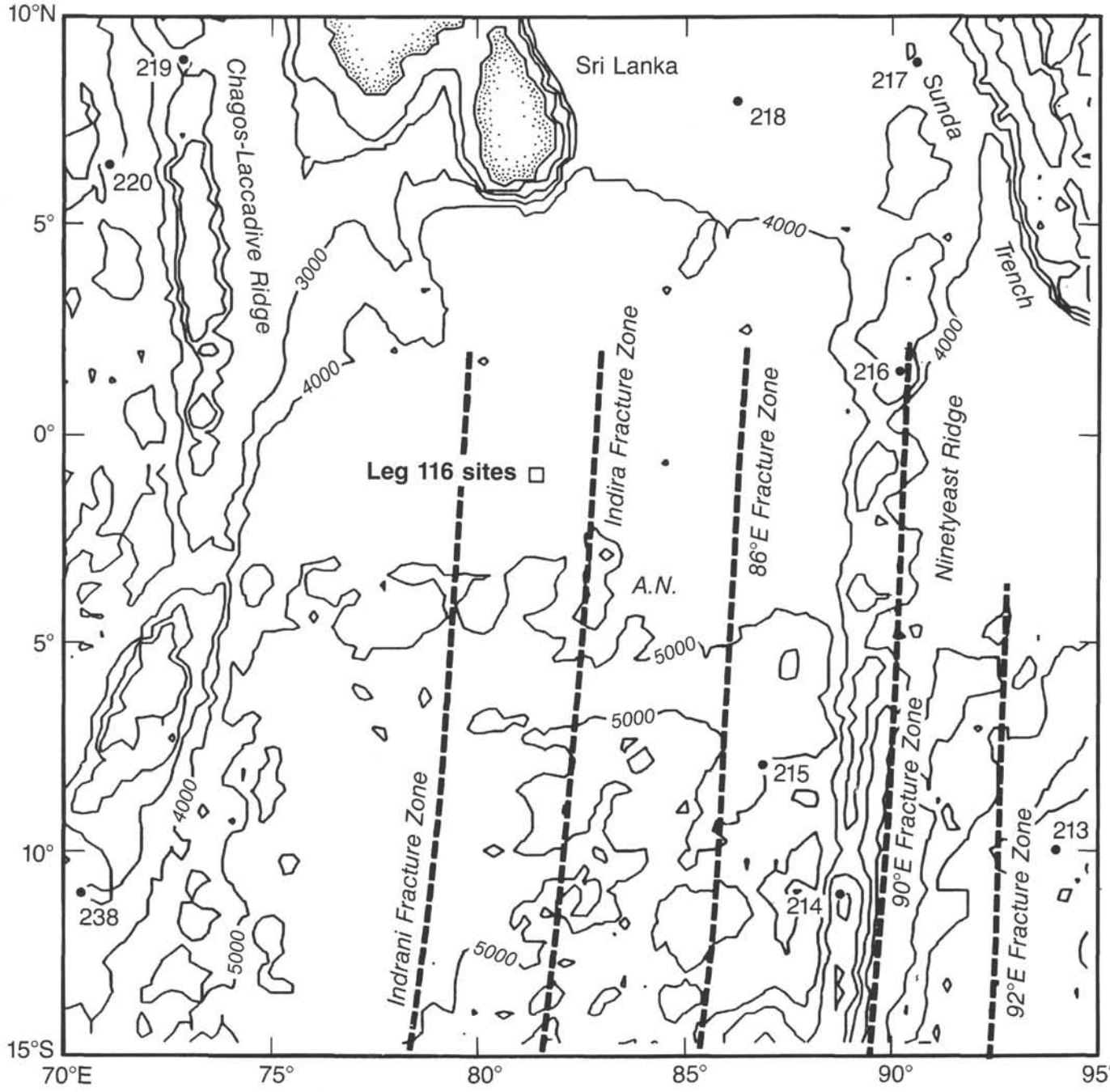

Figure 1. Location map showing position of Leg 116 sites within the north central Indian Ocean. Heavy dashed lines show location of fracture zones and small dots show location of prior DSDP sites. Afanasy Nikiten seamounts are labled A. N. Bathymetry is machine-contoured DBDB-5 gridded bathymetry contoured at 1-km intervals.

be clearly seen, although the quality of these older seismic data is not very good.

The seismic line collected on R/V *Robert D. Conrad* cruise C2706 during the approach to and departure from the site survey is shown in Figure 10. The Leg 116 sites are located on the north slope near the summit of a somewhat subdued long-wavelength undulation. The deformation appears to be best developed several hundred kilometers south of the Leg 116 sites between 5°S and 10°S. It seems to die out gradually to the north toward Sri Lanka; however, the existing seismic data are insufficient to determine whether this is actually the result of the increased sedimentation rate toward the north.

LOCAL SETTING FOR LEG 116 SITES

The site survey for Leg 116 was carried out from June 11 to June 14, 1986, by R/V *Robert D. Conrad* during cruise C2706. The survey consisted of a grid of single-channel seismic reflection lines shot with a water-gun source, run during G.P.S. windows, and heat-flow measurements undertaken during G.P.S.

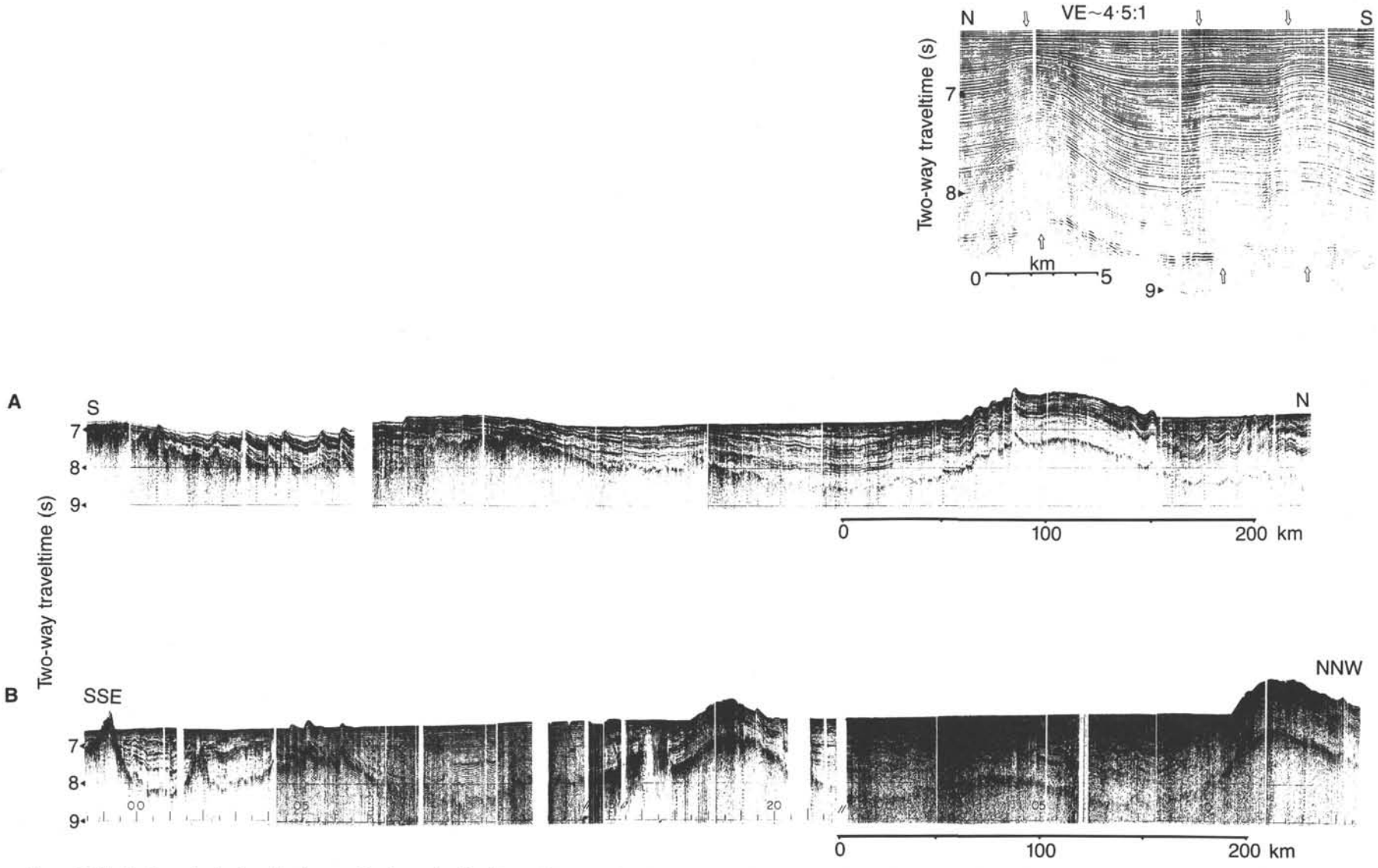

Figure 2. Single-channel seismic reflection profiles from the distal Bengal Fan showing the nature of the long-wavelength basement deformation. Location of tracks is shown in Figure 6 (after Geller et al., 1983).

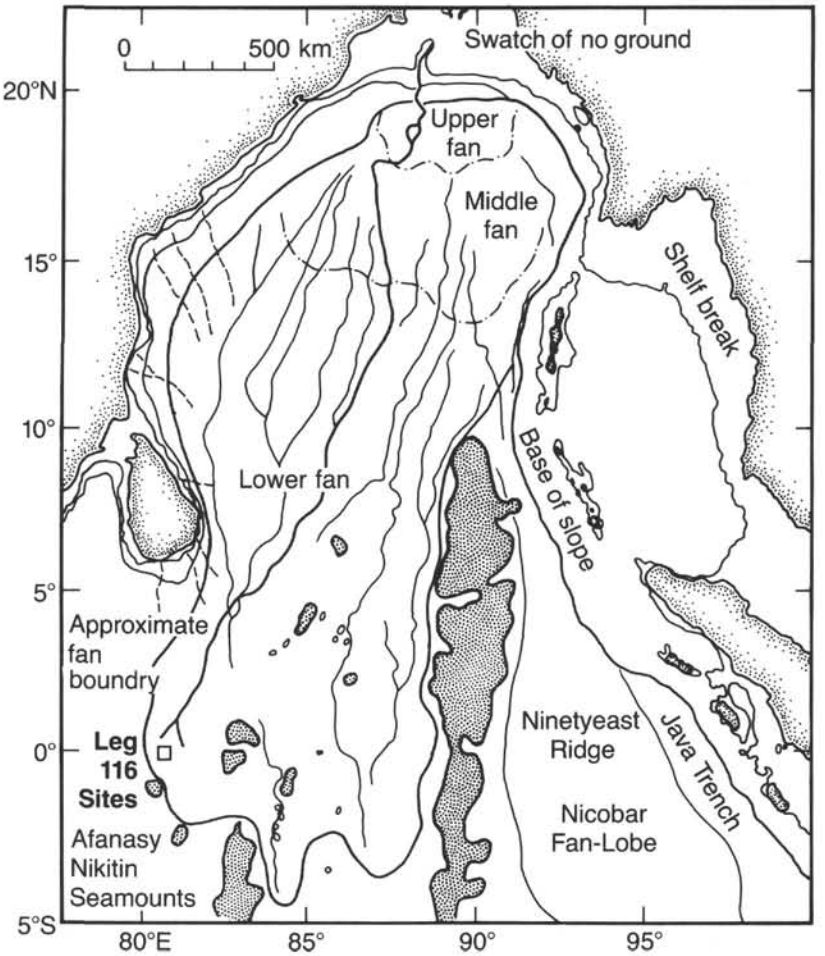

Figure 3. Map of the Bengal Fan showing location of the Leg 116 sites. Indian margin channels and fan channels shown by dashed lines and light lines, respectively; currently active fan channel shown by heavy solid line; seamounts and topographic highs indicated by heavy shading (after Emmel and Curray, 1984).

blackouts. Gravity, magnetic, and 12-kHz echosounder measurements were also collected during underway operations.

The dominant feature of the bathymetry of the Leg 116 site area is a low ridge trending east–west across the site at about 1°03′S (Fig. 11). The ridge separates areas of slightly different depth. Depths to the north range from 4736 to 4727 m and decrease to the south toward the ridge. Depth measurements south of the ridge are fairly uniform in the range of 4744–4746 m. The ridge itself varies in height from 4627 to 4708 m and thus stands roughly 20 to 120 m above the surrounding sea floor.

The seismic reflection lines (Fig. 12) show that the topographic ridge is the surface expression of a nearly vertical fault involving both sediments and basement, which forms the boundary between two apparently tilted fault blocks. This fault, located along the southern edge of the uplifted ridge near 1°4′S, is the southern of three such faults that can be observed in the survey area. The central fault, which is of comparable throw, even though it does not disturb the sea floor, is located about 5 km to the north. The northern fault, which is visible on the three western profiles (B, C, and D) is located 5 to 7 km farther north. It appears to decrease in throw and swing northward from west to east across the survey area.

The seismic reflection lines across the site allow the sediment section to be divided into two first-order acoustic units separated by an unconformity labeled "A" on Figure 12. The lower unit is consistently 1.15 to 1.35 s thick; reflectors within it are parallel and follow the basement. The upper sequence has a maximum thickness of about 0.7 s on the northern of the two fault blocks within the survey area and thins, mainly through pinch-outs, toward the crest of each block. The lower sequence can thus reasonably be interpreted as the predeformation section, and the upper section as the sediments deposited during the deformation. The successive pinching out of reflectors toward the crest of each block suggests that the deformation took the form of rotation of the fault blocks with net uplift of their southern boundaries.

Both seismic sequences exhibit layering, but it is stronger and much more evident in the upper sequence. There is also a difference in the frequency content, with many more high-frequency reflectors in the upper sequence. These differences are not an artifact related to the absorption of energy with depth or to the time varying gain or filters used during processing, because they can be noted both in the troughs and on the crests of the blocks, whereas the thickness of the upper unit can change by more than 0.5 s between the two locations.

The upper seismic unit records a complex history of motion on the faults that varies somewhat from block to block. It includes an upper, highly layered sequence 130 to 200 ms thick that is made up of essentially flat-lying reflectors and has an onlapping relationship with the uplifted sediments at the southern end of each block. This sequence unconformably overlies and truncates reflectors within the underlying sediments. The result-

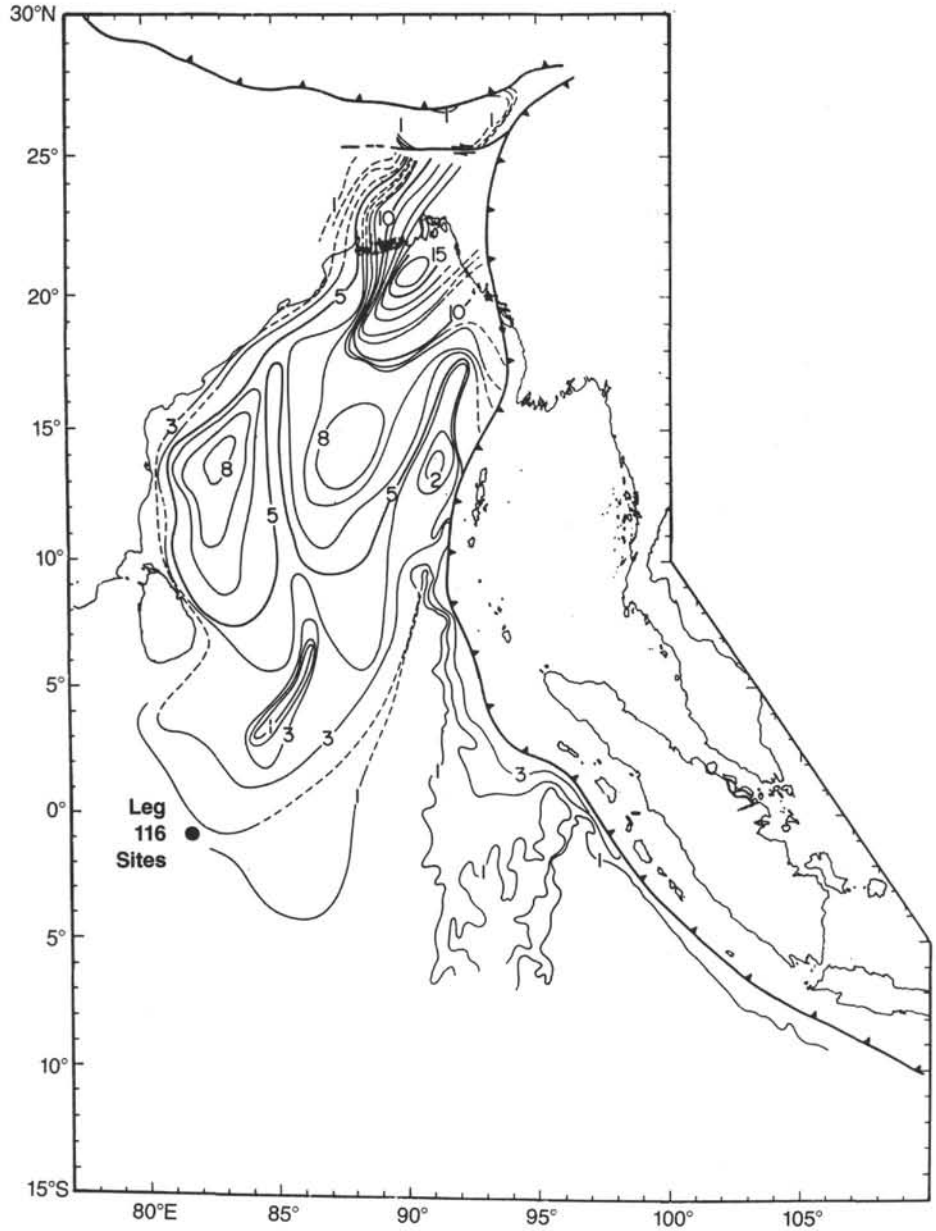

Figure 4. Isopachs of total sediment thickness (km) in the Bengal Fan region (from Curray et al., 1982).

ing unconformity is labeled "B" in Figure 12. The syn-deformational sediments between unconformity "B" and unconformity "A" are characterized by numerous reflectors which are tilted up to the south and commonly terminate by pinching out against underlying reflectors resulting in a thinning of this portion of the section toward the south.

Acoustic basement throughout the survey area has reflection characteristics typical of the top of oceanic crust (Fig. 12). Depth to basement in seconds of two-way traveltime contoured at intervals of 0.05 s is shown in Figure 13. The three faults in the survey area are clearly visible on the depth-to-basement map. The southern two faults appear as zones a hundred to a few hundred meters wide in which basement can not be resolved, while the northern fault is manifest by an abrupt change in the depth to basement. Single-channel migration was employed on the two eastern lines (profiles A and B, Fig. 12) in an attempt to improve the resolution near the fault surfaces. This processing did improve the amount of detail that could be observed in the sections and removed most of the diffractions associated with the faults; however, discrete fault surfaces could not be resolved and the faults still appear as somewhat chaotic zones 4 to 8 shotpoints (190–375 m) wide.

There is a marked variation of the throw on the faults along strike in the 15-km distance mapped during the survey. The northern two faults show a complementary relationship: the throw on the central fault decreases rapidly from around 0.4 s in the eastern part of the survey to slightly more than 0.1 s in the west, whereas the northern fault has a throw of 0.15 s in the east, and increases to almost 0.4 s in the west. This has resulted in a twisting of the fault block between the two faults, so that both the shallowest and deepest depths to basement are found in the eastern end of the survey near the drill sites. The basement at the location of site 717 is almost 8.3 s below the sea surface and is the deepest basement found in the survey area. This

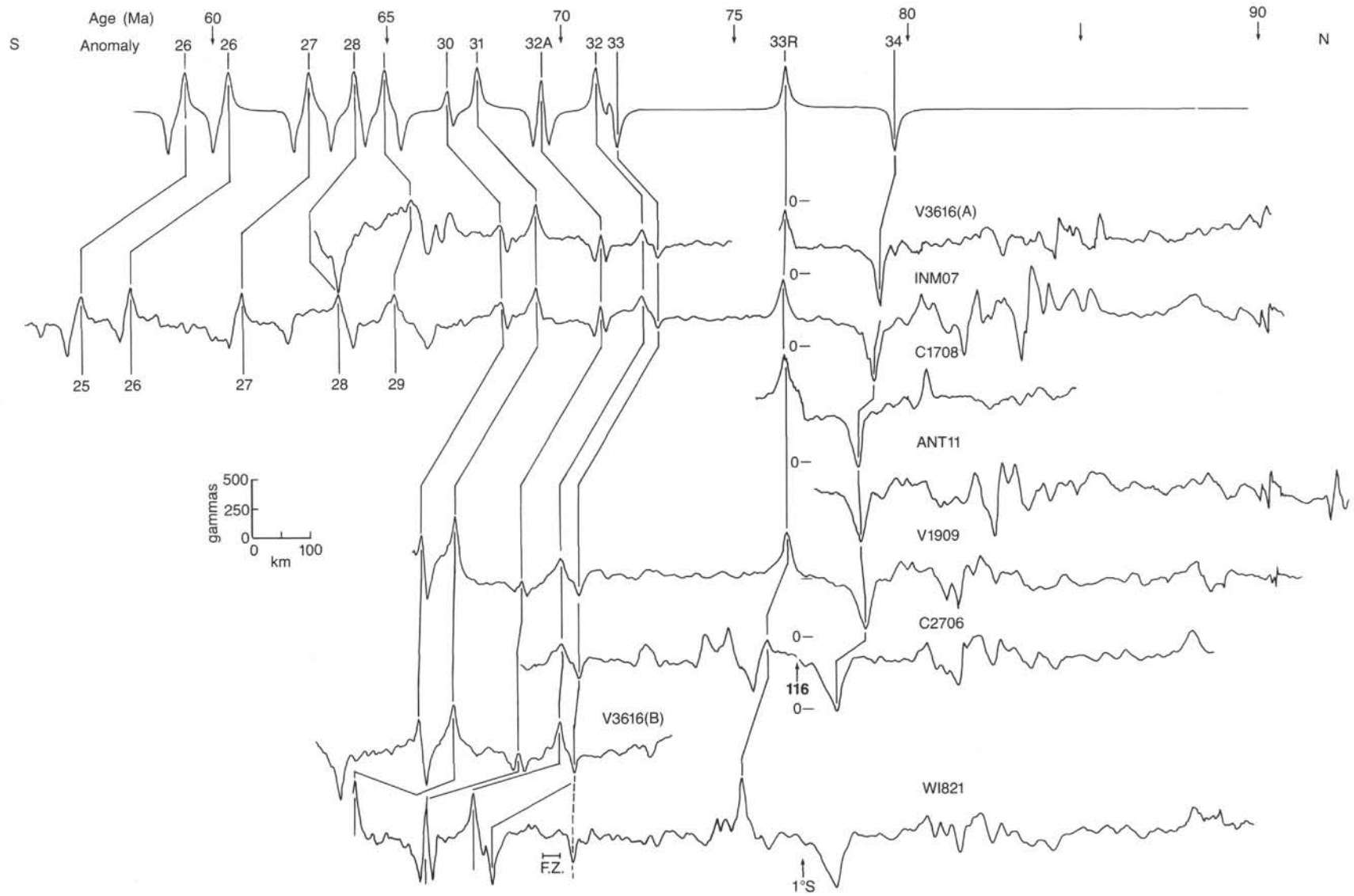

Figure 5. Total intensity magnetic anomaly profiles for north–south lines run between the Indira and Indrani fracture zones. Location of profiles is shown in Figure 6. All profiles are projected along a N–S line with north to the right. Model profile was calculated using the LaBrecque et al. (1977) time scale for a ridge spreading at 6 cm/yr with the anomalies created at 40°S and observed at 5°S. Profile C2706 crosses over the Leg 116 sites at the location noted on the profile.

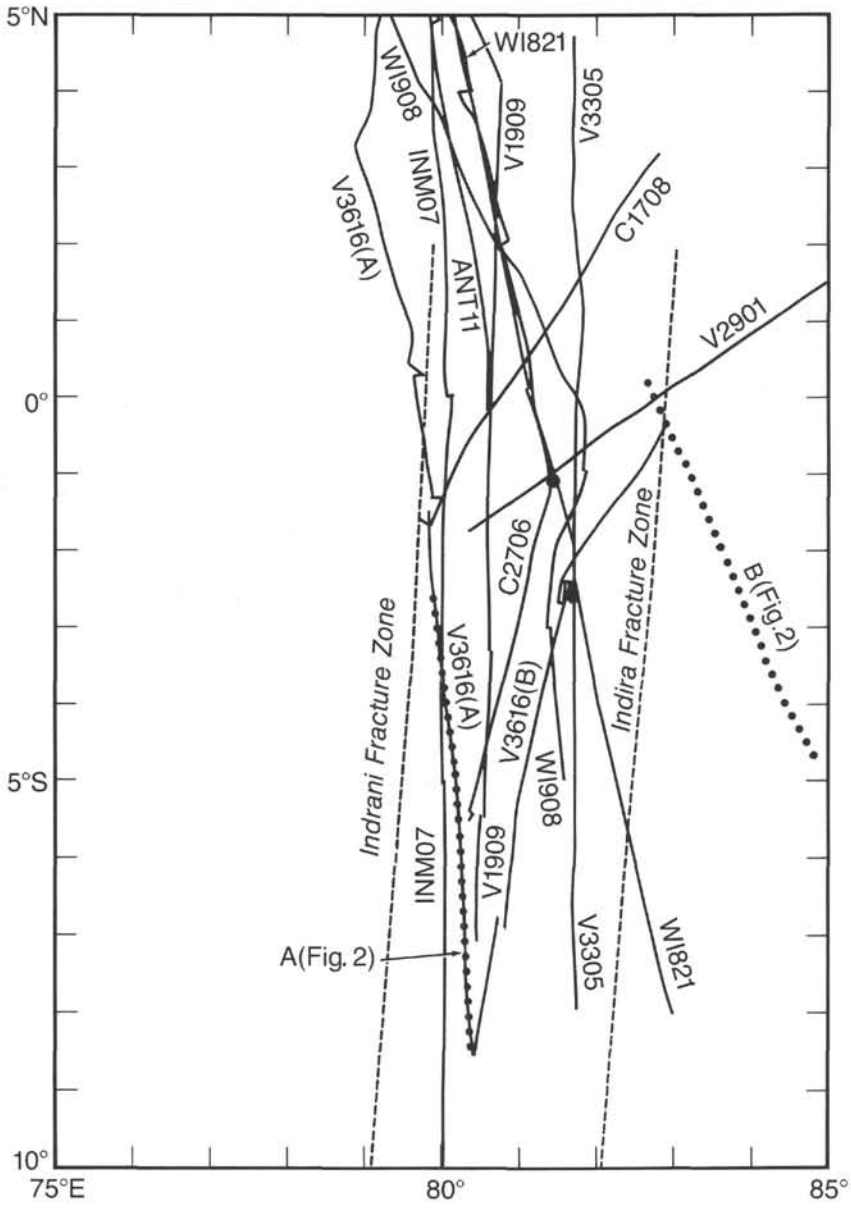

Figure 6. Track chart showing location of geophysical profiles shown in other figures. Dotted tracks are shown in Figure 2.

twisting can also be noted for the southern fault block containing Site 718, but is not nearly as obvious as for the northern block. In this case both the shallowest and deepest depths are found at the western end of the survey region. The southern fault has the largest throw of the three faults surveyed. It varies from about 0.6 s in the west to about 0.4 s in the east. The basement faults are not reflected in the free-air gravity measurements, which maintain a relatively constant level of -58 to -62 mgal throughout the survey area.

The thickest postreflector "A" sediments are found at the location of Site 717 and reach about 0.705 s in thickness (Fig. 14). The thickness of the sediments above reflector "A" decreases to about 0.12 s at the top of that fault block where it is lost in the diffractions associated with the fault. Reflector "A" becomes more horizontal toward the west on the northern fault block, and is found at an intermediate depth of 0.4 to 0.6 s in the western half of the survey.

Reflector "A" becomes somewhat shallower and closer to horizontal, to the east, on the southern fault block, although as is the case with the basement, this tendency is not as obvious as on the northern block. A projection of the reflector southward suggests that it may outcrop near the base of the southern flank of the bathymetric ridge, but it cannot be traced completely under the ridge as a coherent reflector.

The reflectors between the basement and reflector "A" are parallel to the basement. In fact, the thickness of the sediments between the basement and reflector "A" remains constant to within about 0.1 s on each of the fault blocks, but has a different range of values on each block. These ranges are 1.13–1.18 s south of the southern fault, 1.24–1.28 s between the southern and central faults, 1.28–1.38 s between the central and northern faults, and 1.17–1.23 s north of the northern fault. If the sea floor is assumed to have been flat at the onset of deformation, as is probably reasonable, then variation in the thickness of the

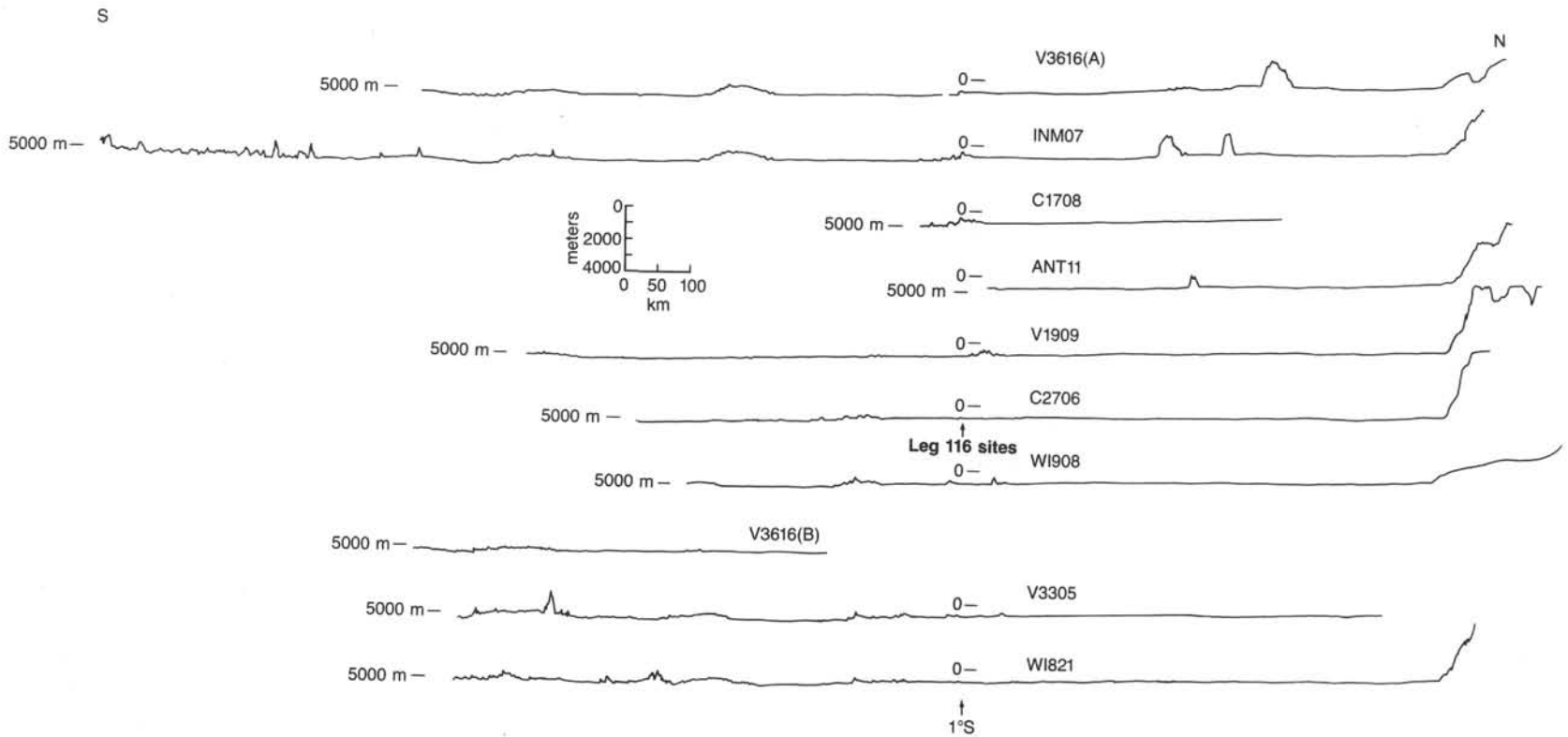

Figure 7. Bathymetry profiles for north–south lines run between the Indira and Indrani fracture zones. Location of profiles is shown in Figure 6. All profiles are projected along a N–S line with north to the right. Profile C2706 crosses over the Leg 116 sites at the location noted on the profile.

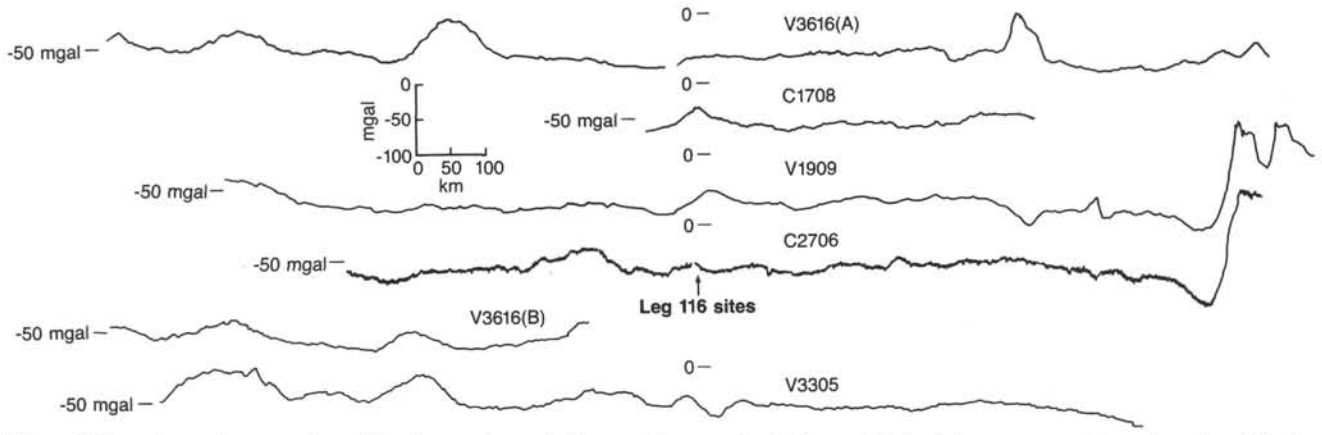

Figure 8. Free-air gravity anomaly profiles for north-south lines run between the Indira and Indrani fracture zones. Location of profiles is shown in Figure 6. All profiles are projected along a N-S line with north to the right. Profile C2706 passes over the Leg 116 sites at the location noted on the profile.

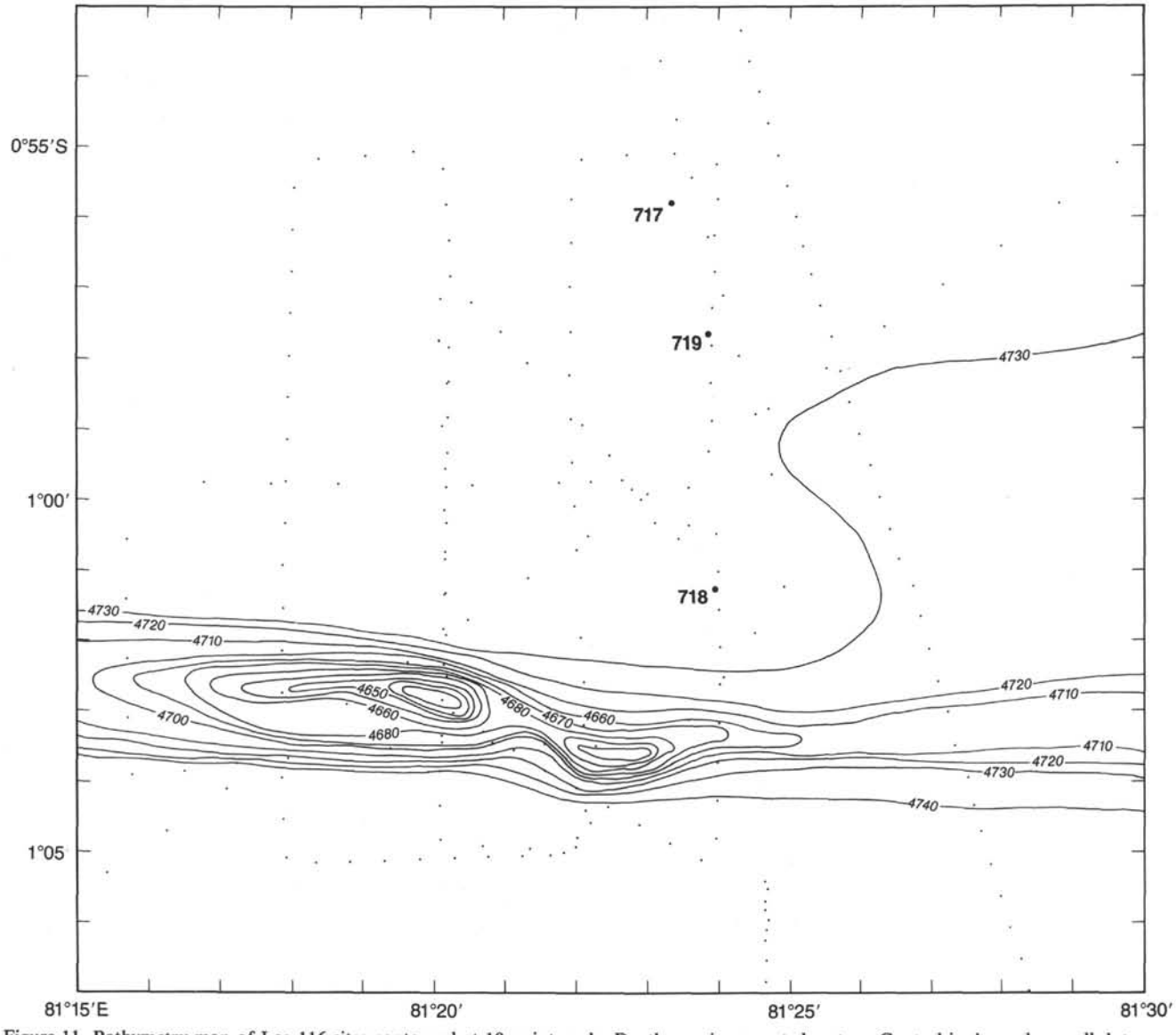

Figure 11. Bathymetry map of Leg 116 sites contoured at 10-m intervals. Depths are in corrected meters. Control is shown by small dots.

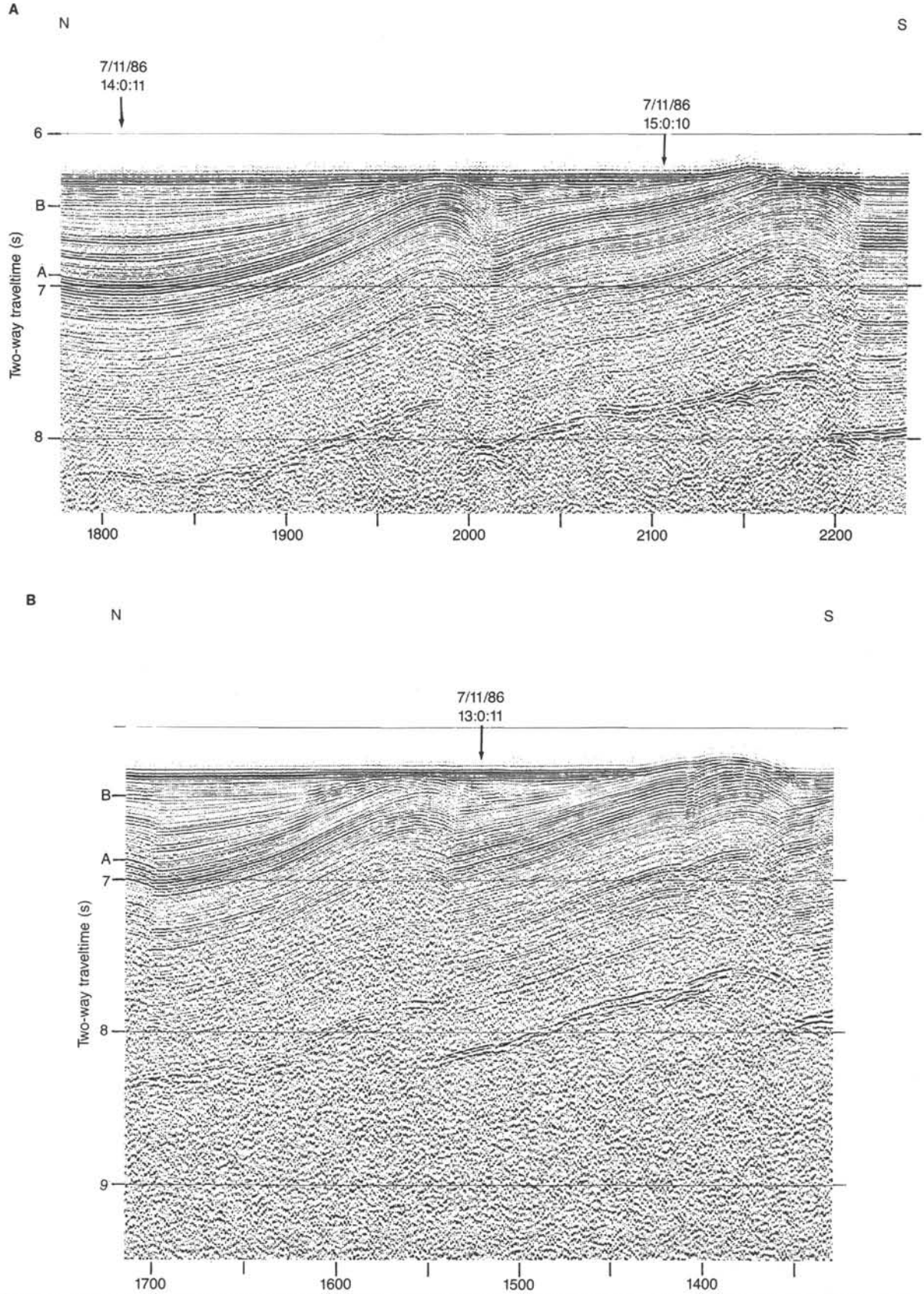

Figure 12. Single-channel seismic reflection lines run during the site survey of Leg 116 sites. These lines are the four north-south lines labeled on Figures 13 and 14. The difference in the appearance of Profiles A and B and of Profiles C and D is due to processing. All four lines were filtered using a time varying band-pass filter, but single-channel migration was applied only to Profiles A and B, which bracket the positions chosen for the drill sites. "A" and "B" are prominent unconformities mentioned in text.

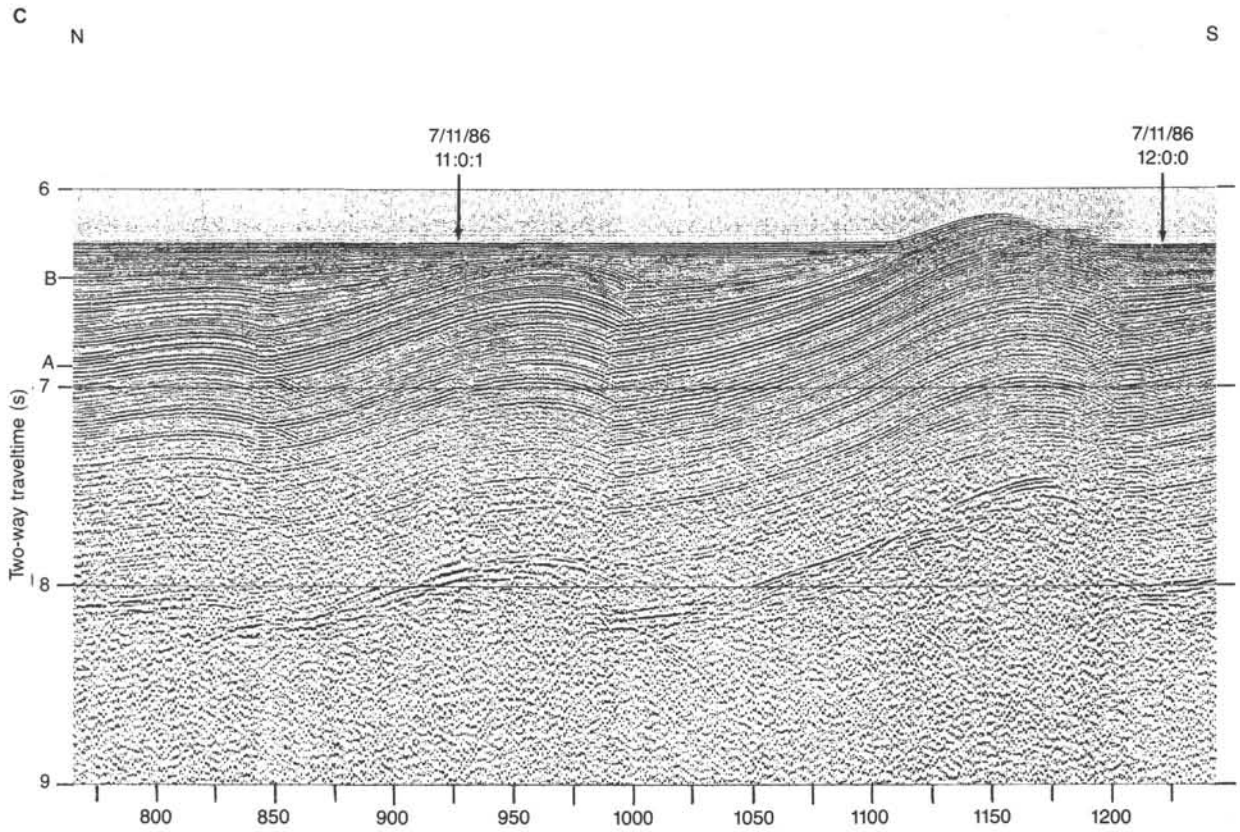

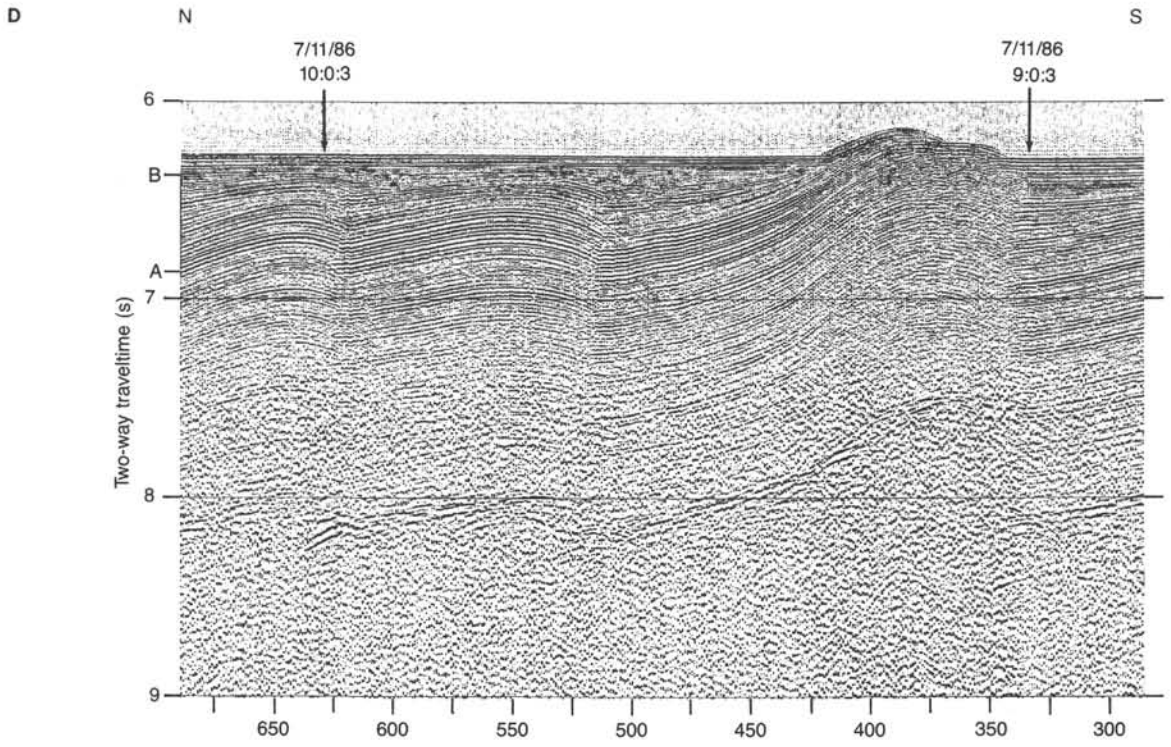

Figure 12 (continued).

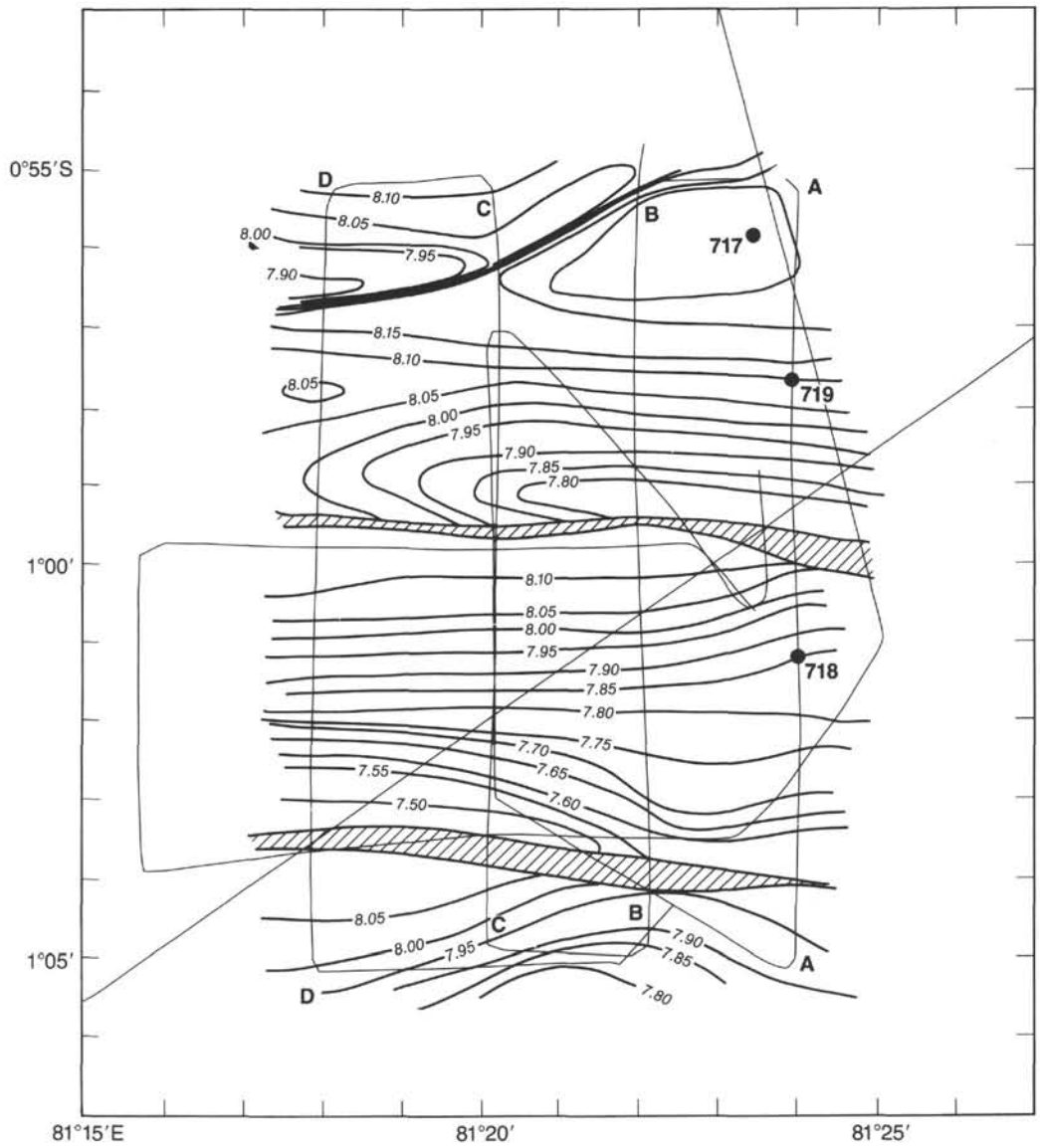

Figure 13. Isopachs of the depth to basement in the vicinity of Leg 116 sites, in seconds of two-way traveltime contoured at 0.05-s intervals. Areas where the basement could not be seen in seismic records are ruled. These regions correspond to the southern and central faults. Control is shown by thin lines.

pre-reflector "A" sediments gives the predeformation basement configuration. The present-day faults appear to have been prominent features on the predeformation basement, implying that they are part of the original fabric of the basement. Their original relief was about 0.05 to 0.1 s (50–100 m). This type of relief and the 5- to 8-km spacing of the faults is typical of the abyssal hill topography found on the East Pacific Rise that is presently spreading at rates comparable to those found in the central Indian Ocean in the Late Cretaceous. It thus appears that the intraplate deformation reactivated the network of small faults created at the ridge crest during the generation of the sea floor.

HEAT-FLOW SURVEY

A heat-flow survey was made as part of the site survey utilizing the Lamont-Doherty Geological Observatory "pogo-probe" apparatus. This instrument consists of five thermistors with an absolute accuracy of better than ± 0.01 °C mounted as outriggers on a 5.5-m long steel spear, with a sixth thermister placed on the core head to measure the bottom-water temperature. Temperature, water pressure, and instrument-tilt data are recorded digitally on magnetic tape and are also transmitted acoustically to the surface. Thermal conductivity values were determined from piston cores using the needle probe technique (von Herzen and Maxwell, 1959).

The measurements consisted of a line of measurements spaced 0.5 to 1.0 km apart extending from about 4 km north of the central fault to about 4 km south of the southern fault, and two shorter lines across the central fault parallel to and on either side of that line (Fig. 15). The 41 heat-flow values range from 44 to 166 mW/m^2 with a mean of 83.7 mW/m^2 and a standard deviation of 21.7 mW/m^2. The theoretically expected heat flow for 78-Ma crust is 53.5 mW/m^2 (Parsons and Sclater, 1977), so that the mean is more than 50% above the expected value. This high mean and the large scatter are both characteristic of the intraplate deformation region (Geller et al., 1983).

The pattern of heat-flow anomalies appears to be oriented in an east–west direction approximately parallel to the faults and to have wavelengths of 1 to a few km between zones of high and

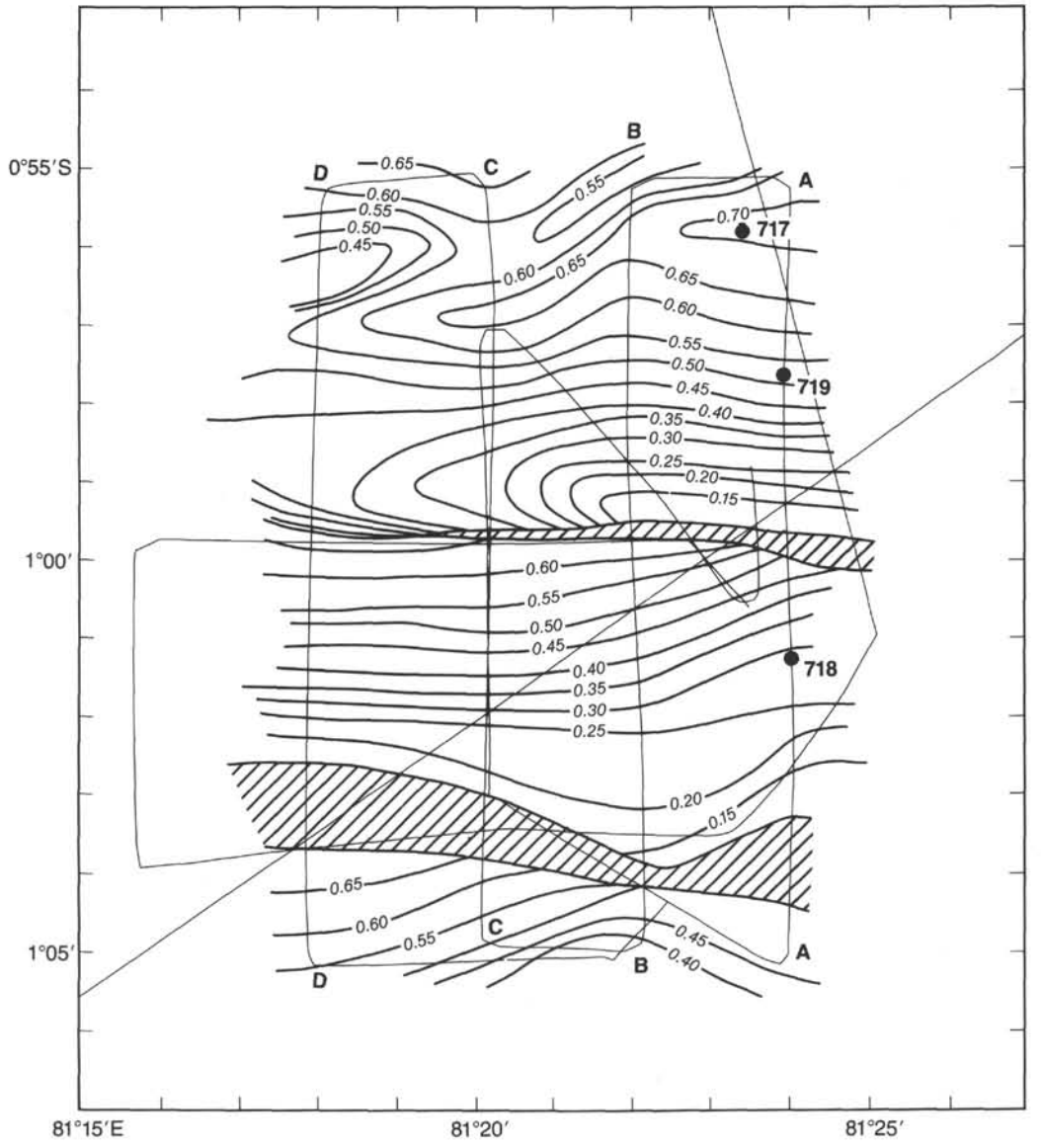

Figure 14. Isopachs of the thickness of sediment between the sea floor and Unconformity "A" contoured at 0.05 s intervals. Areas where Unconformity "A" could not be recognized are ruled. Control is shown by thin lines.

low values (Fig. 15). The presence of such large variations over short distances points to the influence of water flow. The trace of the central fault is not, however, associated with a heat-flow high as might be expected if water is ascending along the fault. Values recorded very near the fault are actually depressed by 20–30 mW/m^2 with respect to surrounding values. The highest values appear to be located about 3 km south of the fault. This suggests that water is not reaching the surface along the fault, but rather may ascend to a certain level along the fault and then flow laterally all along a permeable sediment layer. Site 718 was located on the heat-flow high both to investigate the possible hydrothermal circulation and the effect of the higher thermal gradient on diagenesis and mineralization.

SUMMARY

The Leg 116 sites are located within a small area near 1°S, 81°24′E, approximately halfway between the Indira and Indrani fracture zones on 78-Ma crust within a broad region of the central Indian Ocean that has been undergoing intraplate deformation since the late Miocene. The deformation is recorded in the sediments of the Bengal Fan which were deposited throughout this deformation. The sites are located on two tilted fault blocks resulting from the deformation. The faults bounding the blocks appear to have predated the deformation and to be faults, created at a mid-ocean ridge crest, bounding the abyssal hills formed at a fast-spreading ridge. This preexisting fabric was reactivated during the deformation.

The blocks are not only rotated but are also twisted and thus a considerable variation exists along strike in the throw of the faults and in the depth to basement and to prominent reflectors. The seismic reflection profiles can be divided into two first-order acoustic units separated by an unconformity. In the lower unit, reflectors are parallel to each other and to the basement; the upper unit thins mainly through pinch-outs toward the top of each fault block. This upper syn-deformational unit records the history of motion on the faults.

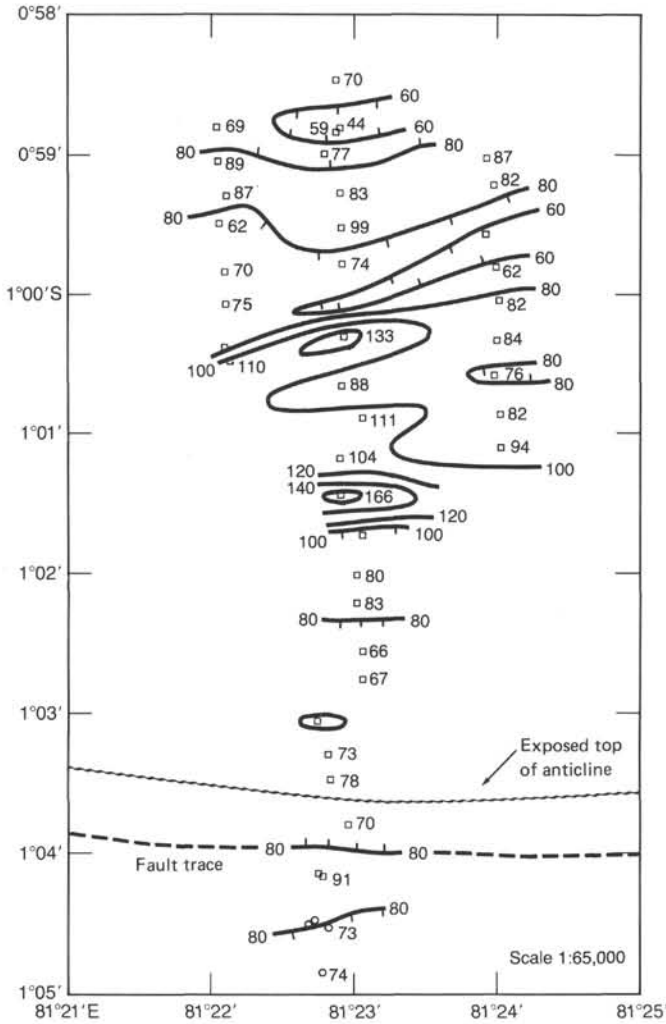

Figure 15. Contour map of heat-flow measurements made during the site survey. Values are in mW/m^2 and contour interval is 20 mW/m^2.

Heat-flow measurements in the survey area show great variability and a mean value significantly higher than that expected for 78-Ma crust. The high variability over short distances suggests that active water circulation is occurring. The fault trace is not associated with a heat-flow high, suggesting that the water is not flowing out of the sediments along the fault but may be spreading laterally through permeable layers within the sediment column.

REFERENCES

Curray, J. R., and Moore, D. G., 1971. Growth of the Bengal deep-sea fan and denudation of the Himalayas, *Geol. Soc. Am. Bull.*, 82: 563–572.

Curray, J. R., Emmel, F. J., Moore, D. G., and Raitt, R. W., 1982. Structure, tectonics and geologic history of the northeastern Indian Ocean. *In* Nairn, A.E.M., and Stehli, F. G. (Eds.), *The Ocean Basins and Margins (Vol 6), The Indian Ocean*: New York (Plenum Press), 399–450.

Eittreim, S. L., and Ewing, J., 1972. Midplate tectonics in the Indian Ocean. *J. Geophys. Res.*, 77:6413–6421.

Emmel, F. J., and Curray, J. R., 1984. The Bengal submarine fan, northeastern Indian Ocean. *Geomarine Lett.*, 3:119–124.

Geller, C. A., Weissel, J. K., and Anderson, R. N., 1983. Heat transfer and intraplate deformation in the central Indian Ocean. *J. Geophys. Res.*, 88:1018–1032.

LaBrecque, J. L., Kent, D. V., and Cande S. C., 1977. Revised magnetic polarity time scale for Late Cretaceous and Cenozoic time. *Geology*, 5:330–335.

Moore, D. G., Curry, J. R., Raitt, R. W., and Emmel, F. J., 1974. Stratigraphic-seismic section correlation and implications to Bengal fan history. *In* von der Borch, C. C., Sclater, J. G., et al., *Init. Repts. DSDP*, 22: Washington (U.S. Govt. Printing Office), 403–412.

Parsons, B., and Sclater, J. G., 1977. An analysis of the variation of ocean floor bathymetry and heat flow with age: *J. Geophys. Res.* 82:803–827.

Sclater, J. G., and Fisher, R. L., 1974. The evolution of the east central Indian Ocean with emphasis on the tectonic setting of the Ninety East Ridge. *Geol Soc. Am. Bull.*, 85:683–702.

Sclater, J. G., Luyendyk, B. P., and Meinke, L., 1976. Magnetic lineations in the southern part of the central Indian Basin. *Geol. Soc. Am. Bull.*, 87: 371–378.

Shipboard Scientific Party, 1974. Site 218. *In* von der Borch, C. C., Sclater, J. G., et al., *Init. Repts. DSDP*, 22: Washington (U. S. Govt. Printing Office), 325–348.

Stein, S., and Okal, E. A., 1978. Seismicity and tectonics on the Ninety East Ridge area: Evidence for internal deformation of the Indian plate. *J. Geophys. Res.*, 83: 2233–2245.

von Herzen, R., and Maxwell, A. E., 1959. The measurement of thermal conductivity of deep-sea sediments by a needle-probe method. *J. Geophys. Res.*, 64: 1557–1563.

Weissel, J. K., Anderson, R. N., and Geller, C. A., 1980. Deformation of the Indo-Australian plate. *Nature*, 287: 284–291.

Ms 116A-108